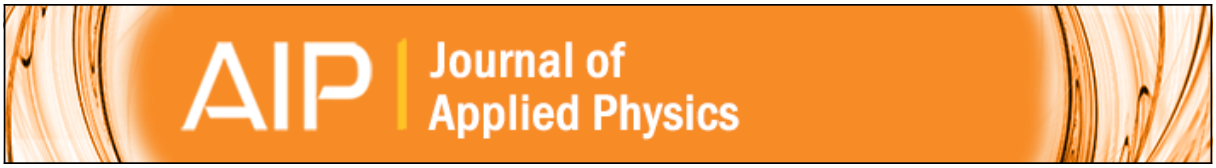

Description of magnetic anisotropy and spin–reorientation transitions in NdFe12x Mo x and NdFe12x Mo x N (x=1.0, 2.0, 3.0)

K. Yu. Guslienko, E. H. C. P. Sinnecker, and R. Grössinger

Citation: Journal of Applied Physics **80**, 1659 (1996); doi: 10.1063/1.362964

View online: http://dx.doi.org/10.1063/1.362964

View Table of Contents: http://scitation.aip.org/content/aip/journal/jap/80/3?ver=pdfcov

Published by the AIP Publishing

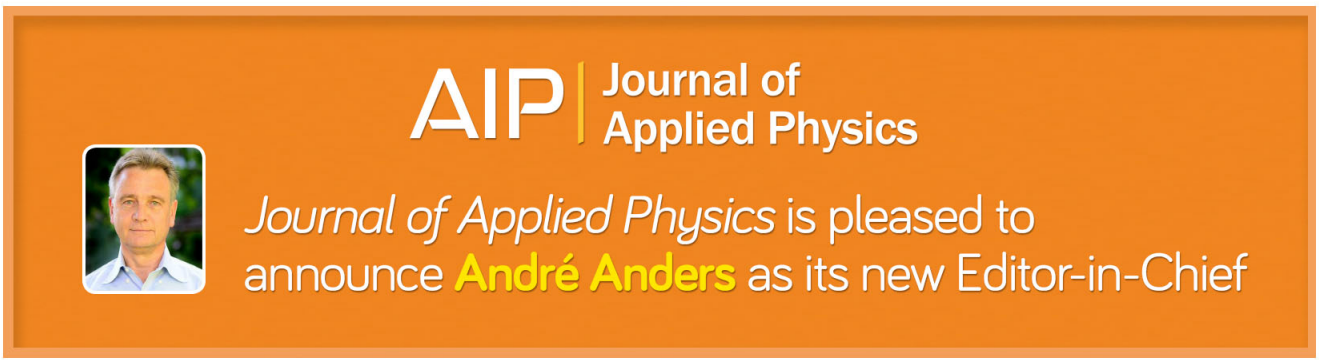

Description of magnetic anisotropy and spin–reorientation transitions in $NdFe_{12-x}Mo_x$ and $NdFe_{12-x}Mo_xN$ ($x=1.0, 2.0, 3.0$)

K. Yu. Guslienko,[a] E. H. C. P. Sinnecker,[b] and R. Grössinger
Institute for Experimental Physics, Technical University of Vienna, Wiedner Hauptstrasse 8-10, A-1040 Vienna, Austria

(Received 1 September 1995; accepted for publication 2 April 1996)

$NdFe_{12-x}Mo_x$ and $NdFe_{12-x}Mo_xN$ ($x=1,2,3$) were investigated by studying the anisotropy field and the temperature or field-induced spin–reorientation transitions. The temperature dependence of the magnetic anisotropy field was determined by means of the singular-point-detection technique for polycrystalline aligned samples. A theoretical explanation of the magnetic anisotropy and the magnetic phase transitions is given. The temperature dependencies of the rare-earth anisotropy constants were calculated using the single-ion model within linear theory. Fitting the experimental data, a set of crystal-field and exchange-field parameters for Nd^{3+} ions was deduced. A first-order spin–reorientation transition from uniaxial to conical phase and a type-2 first-order magnetization process in the perpendicular field are calculated for $NdFe_{11}Mo$. A canted magnetic structure and a type-1 first-order magnetization process in the axial field are predicted for $NdFe_{12-x}Mo_xN$. A change of rare-earth anisotropy after nitrogenation was explained by a bonding charge and a superposition model. The calculated temperature dependence of the anisotropy fields in $NdFe_{12-x}Mo_xN$ is in good agreement with the experimental data over a wide temperature range.
 [S0021-8979(96)09013-5]

I. INTRODUCTION

It is known that the rare-earth (R) contribution to the resultant anisotropy of $R(Fe,M)_{12}$ intermetallics is determined not only by the second-order crystal electric field (CEF) term but also, in general, by the fourth- and sixth-order CEF terms.[1,2] The easy magnetization direction (EMD) can deviate from the c axis due to the high order CEF terms. That is why many temperature- and magnetic-field-induced spin–reorientation transitions are observed in $R(Fe,M)_{12}$ intermetallics, especially with M=Mo,Ti.[1,2] These compounds crystallize in the tetragonal $ThMn_{12}$ structure with the space group $14/mmm$. There is only one type of rare-earth crystallographic site and three crystallographically inequivalent Fe sites ($8f$, $8i$, and $8j$). Nitrogen occupies the octahedral interstitial $2b$ sites adjacent to the R ions.[3] With decreasing temperature the influence of the rare-earth anisotropy increases considerably which leads, in the case of an opposite sign of the R anisotropy and the Fe anisotropy, to a temperature-induced spin–reorientation transition (SRT). The reason for the SRT can be a competition of contributions of different CEF terms to the resulting anisotropy.[1,2] In the $NdFe_{12-x}Mo_x$ series, SRTs occur, but they are absent in the corresponding nitrides within a wide temperature range.[4] It was supposed in Ref. 4 that $NdFe_{12-x}Mo_xN$ shows uniaxial anisotropy. In $NdFe_{11}Mo$ a SRT occurs at $T_s=168$ K, in $NdFe_{10}Mo_2$ it occurs at 147 K,[1,4] and in $NdFe_9Mo_3$ the SRT occurs at 130 K.[4] It has been demonstrated that the absorption of N by rare-earth–iron intermetallics has a dramatic effect on the intrinsic magnetic properties [anisotropy field, Curie temperature (T_C) and total magnetization (M_s)] of $RFe_{12-x}Mo_x$.[4–11] The proposed reason for the T_C and M_s changes is an increase of the Fe–Fe distance due to the increase of the lattice constants respectively the volume of the unit cell.[8] The rare-earth anisotropy changes due to changes of the CEF as described in the frameworks of a bonding charge model[12] and superposition model.[13]

Recent experiments have shown that the best intrinsic magnetic properties, suitable for permanent magnet applications, are found for the nitrides with R=Nd. For instance, at room temperature a coercivity of 8 kOe was achieved in $NdFe_{10}Mo_2N$[6]. In $NdFe_{12-x}Mo_x$ ($x=1,2,3$) a weak uniaxial anisotropy was found whereas after nitrogenation all compounds exhibit a strong uniaxial anisotropy field of about 7–8 T at room temperature.[4] The same results were obtained in $NdFe_{12-x}Mo_xN$ ($x=1$–2.5) with anisotropy fields of 6.4–9.5 T at $T=300$ K (Ref. 6) and for $x=0.8$–2.5 with $H_A=10.7$–16.1 T at $T=1.5$ K.[14]

The contribution to the total magnetic anisotropy from the Fe sublattice favors the c axis in $YFe_{12-x}Mo_x$ for $x\leqslant 2$ (Refs. 1 and 4) (for $x\leqslant 2.5$ in Refs. 10 and 14 and for $x\leqslant 1.5$ in Ref. 9). Room temperature alignment was not successful for $x>2$ (Ref. 9) due to a low value of the uniaxial anisotropy field (low Curie temperature). The observed anisotropy field of $YFe_{9.5}Mo_{2.5}$ at 0.314 T_C is only 0.61 T.[10] The concentration dependence of the saturation moment per formula unit at $T=4.2$ K satisfies approximately the rule $(28.8-8x)\mu_B$ (Ref. 8) and magnetic order should disappear at $x=3.6$. The type of magnetic order and the EMD at high values of x ($x\geqslant 3$) are not clear now. Probably, these compounds are not ferromagnets. A noncollinear magnetic structure was calculated in $YFe_{12-x}Mo_x$ for $x=1,2,3$ in the framework of single-electron band-structure calculations.[15] The EMD in $YFe_{12-x}Mo_xN$ ($x=1$–4) is supposed to be parallel to the c axis over the whole temperature range up to the Curie point.[4] Uniaxial anisotropy in $YFe_{12-x}Mo_xN$ was de-

[a]Permanent address: Inst. Metal Physics, Vernadskogo 36, Kiev-142, Ukraine.
[b]Permanent address: Inst. de Fisica ''Gleb Wataghin,'' Universidade Estadual de Campinas 13083-970, Campinas, S.P., Brazil.

tected for $x=1$ in Ref. 8 and for $x=0.8$, 1, and 1.5 in Ref. 14. But canted ($x=1$) and even planar ($x=2,3$) EMD was reported at room temperature in Ref. 10 and at $T=1.5$ K ($x=2,2.5$) in Ref. 14. Therefore the EMD in the $YFe_{12-x}Mo_xN$ series is under question.

The temperature dependence of the EMD in $NdFe_{12-x}Mo_x$ is more complex due to numerous SRTs. Measuring aligned samples of $NdFe_{12-x}Mo_x$ ($x=0.5$–4) a SRT was observed in Ref. 3 and was thought to be a second-order SRT from ''easy axis'' to ''easy cone.'' Wang *et al.*[16] found two SRTs in $NdFe_{12-x}Mo_x$ within the range $x=1.5$–1.7: easy axis–easy cone 1–easy cone 2. A conical magnetic moment configuration was proposed at a temperature below T_s (Ref. 16) and $x<1.5$. If $x>1.7$ an easy-axis phase is absent up to the Curie temperature and only a SRT between two canted magnetic structures exists.

Nitrogen modifies the CEF experienced by the $4f$ shell of the R ions. It is expected[12] from the bonding-charge model calculation that nitrogenation in $NdFe_{11}Ti$ leads to a considerable increase of A_{20} up to $+370\ Ka_0^{-2}$. The same influence of nitrogenation on A_{20} is expected for isostructural $NdFe_{12-x}Mo_x$ compounds because high values of the anisotropy fields were measured.[4] But in these compounds the contributions of high order CEF parameters should also have considerable values. No spin reorientation was observed in $NdFe_{12-x}Mo_xN$[3] below room temperature. The results[6] obtained using x-ray diffraction patterns of magnetically aligned powders show that all nitrides exhibit nearly an easy c-axis anisotropy at room temperature.

Due to the complex behavior of the magnetic anisotropy, the type of the SRT and directions of the EMD in nearly all $NdFe_{12-x}Mo_xN$ and $NdFe_{12-x}Mo_x$ are not clear up to now. The crystal field and exchange field parameters are unknown. The question about the existence of first-order magnetization processes (FOMPs) in $NdFe_{12-x}Mo_xN$, which were recently observed in isostructural $PrFe_{12-x}Mo_xN$,[10] is open.

In the present article the experimentally observed temperature dependence of the anisotropy fields $H_A(T)$[4] and additionally the Curie and SRT temperatures are used in order to find crystal and exchange field parameters for $NdFe_{12-x}Mo_x$ and $NdFe_{12-x}Mo_xN$ within the single-ion rare-earth anisotropy model. To determine the Fe contribution to the resulting magnetic anisotropy the anisotropy fields of the isostructural compounds $YFe_{12-x}Mo_xN$. $YFe_{12-x}Mo_x$ were measured over a wide temperature range using the singular-point-detection (SPD) technique. The experimental procedures are described in Sec. II. In Sec. III the details concerning the anisotropy and FOMP field calculations in the framework of the linear theory are given. An explanation of the magnetic anisotropy and SRT in these compounds is given on the basis of the found model parameters and CEF superposition model in Sec. IV. A summary is presented in Sec. V.

II. EXPERIMENTAL DETAILS

Polycrystalline $YFe_{12-x}Mo_x$ samples were prepared by induction melting the stoichiometric amounts of the constituents under argon atmosphere. Starting materials of 99.99 wt % purity were used. The ingots were remelted four times to achieve homogeneity. The as-cast ingots were wrapped in Ta foil and sealed in a pre-evacuated and then argon gas filled quartz tube, followed by annealing at 1373 K for four weeks. The annealed samples were then water quenched and their phase content was checked by x-ray diffraction using Co $K\alpha$ radiation. All obtained samples showed a main phase with the tetragonal $ThMn_{12}$ structure. Traces of elemental Fe were detected in all samples (below 5%).

The fine-powdered particles were nitrided at 723 K for 10 h under a nitrogen gas pressure of 5 bar. The amount of the nitrogen absorbed by the samples was obtained by the difference in weight of the samples before and after the nitrogenation.

Magnetically aligned samples of cylindrical shape were prepared by aligning fine powder particles (the diameter is smaller than 40 μm) at room temperature applying a magnetic field of about 1.5 T perpendicular to the cylinder axis. Their directions were fixed with epoxy resin.

The temperature dependence of the magnetic anisotropy field $H_A(T)$ was determined by means of the SPD technique in a pulsed-field magnetometer which can be operated from 4.2 to 1000 K with a maximum field of 30 T. Polycrystalline aligned samples of $YFe_{12-x}Mo_xN$ and $YFe_{12-x}Mo_x$ ($x=1,2,3$) were used for the measurements. H_A and FOMP fields are detected from the second and the first derivatives of the magnetization curve with respect to the magnetic field by the SPD technique.

III. METHOD OF CALCULATION

Within the framework of a two-sublattice model of the rare-earth (R)–transition metal (T) ferrimagnets the R sublattice and T sublattice contributions to the resulting magnetic anisotropy can be calculated.

For calculating the temperature dependence of the rare-earth anisotropy constants the single-ion model was used. A detailed description of this model was given in Refs. 1 and 2. A two-sublattice molecular-field theory was used to describe the temperature dependence of the R-sublattice magnetization. For the tetragonal symmetry of the $ThMn_{12}$ structure only the crystal field parameters A_{20}, A_{40}, A_{44}, A_{60}, and A_{64} are necessary according to the symmetry of the crystal. The single-ion rare-earth Hamiltonian for a ground state multiplet with an angular momentum J can be written as

$$H_R=H_{\mathrm{ex}}+H_{\mathrm{CF}}+H_Z, \tag{1}$$

where $H_{\mathrm{ex}}=2(g_J-1)\mu_B\mathbf{J}\cdot\mathbf{H}_{\mathrm{ex}}$ describes the isotropic exchange coupling energy with the iron sublattice, $H_{\mathrm{CF}}=\Sigma\theta_n A_{nm}C_m^n(\mathbf{J})$ is the crystal field Hamiltonian decomposed by irreducible tensor operators $C_m^n(\mathbf{J})$, θ_n are the Stevens factors, and $H_Z=g_J\mu_B\mathbf{J}\cdot\mathbf{H}$ describes the Zeeman energy in an external magnetic field.

The total free energy consists of Fe and R contributions and is given by

$$\begin{aligned} F&=-k_BT\ \ln Z_R+K_{1\mathrm{Fe}}\sin^2\theta-\mathbf{M}_{\mathrm{Fe}}\cdot\mathbf{H},\\ Z_R&=Sp[\exp(-\beta H_R)],\quad \beta=1/(k_BT), \end{aligned} \tag{2}$$

where $K_{1\mathrm{Fe}}$ and $\mathbf{M}_{\mathrm{Fe}}$ are the anisotropy constant and magnetic moment of the Fe sublattice per formula unit, respec-

tively. We assumed that the Fe sublattice can be described by only the first anisotropy constant and the global Fe magnetization, that is a sum of the Fe contributions (local magnetic moments may be noncollinear) from $8i$, $8j$, and $8f$ sites. The reason for this is the dominant role of the Fe–Fe isotropic exchange in comparison with the magnetic anisotropy for these compounds. The values of $K_{1\mathrm{Fe}}$ and M_{Fe} are assumed to be the same as those found in $YFe_{12-x}Mo_xN$, $YFe_{12-x}Mo_x$ after scaling for the different Curie temperatures. It is not correct to neglect the change of Fe-sublattice anisotropy upon nitrogenation as in Ref. 13 because strong nitrogen influence on $K_{1\mathrm{Fe}}$ and M_{Fe} exists. To estimate $M_{\mathrm{Fe}}(T)$ an approximation[17]

$$M_{\mathrm{Fe}}(T)/M_{\mathrm{Fe}}(0)=(1+b)(1-T/T_C)^{1/2}-b(1-T/T_c) \tag{3}$$

with different $M_{\mathrm{Fe}}(0)$ and the fitting coefficient b was used.

The values $K_{1\mathrm{Fe}}(T)$ for $YFe_{12-x}Mo_xN$, $YFe_{12-x}Mo_x$ were calculated over a wide temperature region using the formula $K_{1\mathrm{Fe}}(T)=K_{1\mathrm{Fe}}(0)(1-\alpha T/T_C)\sigma^3(T)$, where $\sigma(T)=M_{\mathrm{Fe}}(T)/M_{\mathrm{Fe}}(0)$. The coefficients α and the values of $K_{1\mathrm{Fe}}(0)$ were found from a least-squares fitting procedure using the equation $K_{1\mathrm{Fe}}(T)=\mu_0 H_A(T)M_{\mathrm{Fe}}(T)/2$ giving the temperature dependence of $K_{1\mathrm{Fe}}(T)$. The anisotropy fields $H_A(T)$ for $YFe_{12-x}Mo_xN$, $YFe_{12-x}Mo_x$ were determined by the SPD technique within a temperature region of 10–293 K (Fig. 1). A correction for the demagnetizing field was done. The Fe-ion magnetic moment decreases with increasing Mo concentration x, the Fe-anisotropy constant has a maximum value $K_{1\mathrm{Fe}}(4.2\ \mathrm{K})=13.3$ K/f.u. for $x=2$ in $YFe_{12-x}Mo_xN$ and 25.7 K/f.u for $x=1$ in $YFe_{12-x}Mo_x$ which are comparable with that found in $YFe_{11}Ti$.[2]

The experimental data obtained by the SPD technique on polycrystalline and magnetically aligned samples will be used in the present investigation. The contribution of the basal plane anisotropy constants K_2', K_3' are reduced to zero by averaging the azimuthal angle. Therefore the basal plane anisotropy (given by the A_{44}, A_{64} crystal field parameters) does not contribute to the measured anisotropy field or to the FOMP critical field. The temperature dependence of $H_{\mathrm{ex}}(T)$ is supposed to be proportional to $M_{\mathrm{Fe}}(T)$. We used the expression $H_{\mathrm{ex}}(T)=H_{\mathrm{ex}}(0)\sigma(T)$. The resulting anisotropy constants are $K_1=K_{1\mathrm{Fe}}+K_{1\mathrm{R}}$, $K_2=K_{2\mathrm{R}}$, $K_3=K_{3\mathrm{R}}$. For Nd–Fe intermetallics the total magnetization is $M_s=M_{\mathrm{Fe}}+M_{\mathrm{R}}$, where $M_{\mathrm{R}}(T)=M_{\mathrm{R}}(0)B_J(\xi)$ and $M_{\mathrm{R}}(0)=g_J J$ is the free R^{3+} rare-earth ion value.

The total anisotropy field is given by $H_A=2(K_1+2K_2+3K_3)/M_s$,[1,2] where M_s is the total magnetization. This equation is valid for $NdFe_{12-x}Mo_xN$ over the whole temperature range of $H_A(T)$ as determined by the SPD technique. The measured peak in $\partial^2 M_s/\partial t^2$ by the SPD method has a sharp maximum (cusp) at $H=H_A$. The temperature dependence of H_A was calculated by fitting the experimental data over a wide temperature range.

To calculate the temperature dependence of the rare-earth anisotropy constants a first-order perturbation theory is used.[1] In order to estimate the accuracy of this linear theory we calculated the second-order correction at finite temperature[1] under supposition that the second-order CEF term (A_{20}) gives the leading contribution to the rare-earth anisotropy constants and to the anisotropy field. Thus we get the second-order correction to the anisotropy field in the form $H_A(T)=H_A^{\mathrm{linear}}(T)[1+\epsilon(T)]$, where the relative error of the linear theory $\epsilon(T)$ depends strongly on the temperature. Calculating the matrix elements of H_{CF}, $\epsilon(T)$ can be written as follows:[1]

$$\epsilon(T)=-\frac{3}{8}\frac{A_{20}}{T_{\mathrm{ex}}}f_J(t,T_{\mathrm{ex}}/T_C),\quad t=T/T_C,$$
$$T_{\mathrm{ex}}=2\mu_B H_{\mathrm{ex}}(0). \tag{4}$$

The second-order correction is determined by the ratio A_{20}/T_{ex} as well as the function $f_J(t)$ which depends strongly on the temperature and on J. When the temperature increases, the absolute value of the function $f(t)$ decreases and therefore the second-order corrections to the anisotropy field calculated within the linear theory decreases rapidly. The crystal field parameters found within the linear theory will be effective parameters if $H_{\mathrm{CF}}\ll H_{\mathrm{ex}}$ is not fulfilled and ϵ is not small compared with unit.

A field-induced FOMP occurs due to the existence of two relative minima of the free energy. Following Ref. 18 two types of FOMP can be distinguished: transition to the saturated state (type 1) or to a not-saturated state (type 2). In the frameworks of the linear theory of R anisotropy the high order CEF parameters are necessary to describe a FOMP. FOMPs are observed at low temperatures when K_2, K_3 are not negligible. The analysis of the total free energy (2) and its derivatives with respect to the magnetization angle θ delivers an analytical solution for the critical magnetization and critical FOMP field in axial fields and perpendicular to the c-axis magnetic fields.[18]

Charge transfer takes place from R ions to N atoms because their electronegativities differ sufficiently.[12] In the framework of the superposition model,[19] nitrogenation leads to additional contributions to the CEF parameters so that the surrounding R-ions electron charge density changed:

$$A_{nm}=\sum_j (-1)^m b_n(R_j)C^n_{-m}(\Theta_j,\Phi_j), \tag{5}$$

where b_n are the intrinsic model parameters, $C^n_m(\Theta,\Phi)=[4\pi/(2n+1)]^{1/2}Y^m_n(\Theta,\Phi)$ are the irreducible tensor operators connected with the spherical harmonics Y^m_n, R_j, Θ_j, Φ_j are the spherical coordinates of neighbor N atoms, j is the number of the site which are occupied by the N atoms.

In the $ThMn_{12}$ structure N atoms occupy the octahedral $2b$ sites.[3,12] Every Nd ion has two $2b$-site neighbors ($j=1,2$). Their coordinates are $R_1=R_2=R=c/2$, $\Theta_1=0$, $\Theta_2=\pi$. The latter means that only axial contribution from $2b$ sites to CEF on the R sites are present due to $C^n_m(\Theta,\Phi)=\delta_{mo}P_n(\cos\Theta)$ at $\Theta=0,\pi$. Using $P_n(\mp 1)=1$ we get under supposition that the $2b$ sites are fully occupied

$$A_{nm}=b_n(R)\sum_j (-1)^m\delta_{mo}P_n(\cos\Theta_j)|_{\Theta_j=0,\pi}$$
$$=2b_n(R)\delta_{mo}, \tag{6}$$

where $P_n(x)$ are the Legendre polinoms.

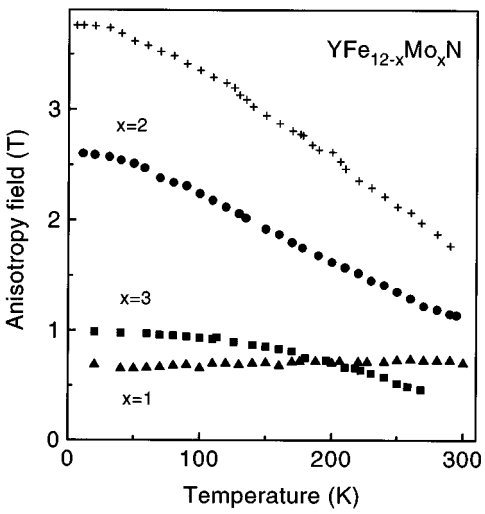

FIG. 1. Temperature dependencies of the anisotropy fields for $YFe_{12-x}Mo_xN$ and $YFe_{11}Mo$ [the crosses (+)].

The superposition model parameters b_n can be calculated, for instance, by the point charge model as $b_n(R) = -e^2Q\langle r^n\rangle/R^{n+1}$. Q is an effective charge located on the N-atom site caused by the transferred electrons. $b_n(R)$ describes the contribution to the n-order CEF parameter from a single nitrogen atom. If the N concentration on the interstitial sites is c_N then the nitrogen contribution in the CEF parameters for $R(Fe,M)_{12}N$ compounds can be written as $A_{no} = 2c_N b_n(R)$.

IV. RESULTS AND DISCUSSION

The experimental data for $YFe_{12-x}Mo_xN$ and $NdFe_{12-x}Mo_xN$ ($x=1,2,3$) obtained in Ref. 4 and in the present article are explained by the models described above. The measured anisotropy fields $H_A(T)$ for $YFe_{12-x}Mo_xN$ (Fig. 1) were used to find the Fe-anisotropy constant and to separate the N influence on the Fe and Nd sublattices.

A. $YFe_{12-x}Mo_xN$ and $YFe_{12-x}Mo_x$

The anisotropy fields measured by the SPD technique for $YFe_{12-x}Mo_xN$ and $YFe_{11}Mo$ are shown in Fig. 1. The possible cause of an anomalous temperature dependence and the low values of $H_A(T)$ for $YFe_{11}MoN$ (Fig. 1) may be a competition of contributions from different Fe sites to the resulting Fe-anisotropy constant.[6,20] Mo substitutes for Fe preferably on $8i$ and $8f$ sites,[3] which contribute to the total K_{1Fe} both positive and negative. Uniaxial anisotropy in $YFe_{11}MoN$ was detected in Refs. 8 and 14. The cusp of $\partial^2M/\partial H^2(\partial^2M/\partial t^2)$ vs H measured in the present article for $YFe_{12-x}Mo_xN$ means that the ''hard plane'' anisotropy exists.[21] This is possible only for the easy axis and easy cone (which is forbidden without high order Fe-anisotropy constants) types of magnetic anisotropy and has no sense for easy plane anisotropy. Therefore the measured EMD of $YFe_{12-x}Mo_xN$ ($x=1,2,3$) is interpreted as easy axis. From this point of view the conclusion given by Refs. 10 and 14 about the existence of an easy plane anisotropy in $YFe_{12-x}Mo_xN$ for $x>1.5$ is not clear because the last should lead to a discontinuous slope of $\partial^3M/\partial H^3$.[21] Also, to align the easy plane samples[14] it is necessary to use a special rotational technique.

In addition, very short heat treatment (annealing) was used in Ref. 10, which could cause Mo atoms to occupy not-equilibrium sites in the lattice, whereas the global Fe anisotropy depends strongly on the distribution of Fe and Mo over $8i$, $8j$, and $8f$ sites. To estimate the K_{1Fe} values the individual site anisotropy (ISA) model[22] can be used. Within the ISA model

$$K_{1Fe}(x) = \sum_i n_i f_{iFe}(x) K_{1Fe}^{(i)}, \tag{7}$$

where n_i is the number of equivalent sites occupied by the Fe and Mo ions in a unit cell, $f_{iFe}(x)$ are the occupancy factors of Fe on the i sites when the Mo concentration is x, $K_{1Fe}^{(i)}$ are the local Fe contribution to the first anisotropy constant from the individual i sites.

Applying Eq. (7) for the $ThMn_{12}$ structure with $K_{1Fe}^{(i)}$ taken from Ref. 22 and $f_{iFe}(x)$ taken from neutron-powder-diffraction experiments[3] for $x=1,3$, we got $K_{1Fe}(1)>0$, $K_{1Fe}(3)>0$ for $YFe_{11}Mo$, $YFe_{11}MoN$, and YFe_9Mo_3N. This agrees qualitatively with the present measurements and calculations, by which the uniaxial EMD is expected for these compounds. The calculated $K_{1Fe} = 23.1$ K/f.u. for $YFe_{11}Mo$ agrees well with our value $K_{1Fe}(4.2\ \text{K})$. $K_{1Fe}(x)$ decreases rapidly with increasing x for $YFe_{12-x}Mo_x$ and the anisotropy field is not detectable applying the SPD for $x=3$. The occupation factors $f_{iFe}(x)$ after nitrogenation are the same as in the host compounds[3] and K_{1Fe} changes due to a change of the local contributions $K_{1Fe}(8i)$, $K_{1Fe}(8f)$. The ISA model does not allow us to calculate temperature dependence of the $K_{1Fe}^{(i)}$ and, therefore, the temperature dependence of $K_{1Fe}(x)$ whereas it is possible for the rare-earth anisotropy constants within the single-ion CEF model.

B. $NdFe_{11}MoN$ and $NdFe_{11}Mo$

Fitting the experimental data of $H_A(T)$ for $NdFe_{11}Mo$ a set of Nd^{3+}-ion parameters are deduced: $T_{ex}=532$ K, $A_{20}=-167$ K, $A_{40}=-13$ K, $A_{60}=211$ K (Table I). T_{ex} is comparable with that of $NdFe_{11}Ti$.[2] From our experimental data[4] it is evident that $H_A(T)$ is small. The equation (3) $K_1(T_s)K_3(T_s)=K_2^2(T_s)$ and the experimental values of $H_A(T)$ were used for the fits. The calculated cone angle $\theta_c(T)$ in $NdFe_{11}Mo$ exhibits with decreasing temperature a jump and the SRT detected at $T_s=147$ K (Ref. 4) is of first order. The same SRT was calculated for isostructural intermetallic $NdFe_{11}Ti$ in Ref. 2. The kind of SRT differs from that supposed in Ref. 4. The present set of the Nd^{3+} crystal field parameters leads to the prediction of a type-2 FOMP in perpendicular magnetic fields at low temperatures. But the FOMP field is small (<0.7 T). This may be the reason why this FOMP was not detected in Ref. 4.

With the fitted crystal-field parameters the anisotropy constant K_2 is negative due to the considerable value of $\Theta_6<0$ and K_3 is positive over the whole temperature range for $NdFe_{11}Mo$. The Fe sublattice and the CEF parameter A_{60} gives a positive contribution to $K_1(T)$. The first anisotropy

TABLE I. Fitted crystal-field parameters for $NdFe_{12-x}Mo_xN$ and $NdFe_{12-x}Mo_x$. The units of $T_{ex}=2\,\mu_B\,H_{ex}(0)$, T_s and A_{nm} are K*—taken from Ref. 1. A–C are the ''easy axis''—''easy cone'' SRT. A-1(2), P-1(2) denote the type 1(2) FOMP in axial and perpendicular fields, respectively. T_s are taken from Ref. 4.

	T_{ex}	A_{20}	A_{40}	A_{60}	T_s	SRT	FOMP	Remarks
$NdFe_{11}Mo$	532	−167	−13	211	168	A–C	P-2	First-order SRT
$NdFe_{11}MoN$	1140	51	−611	710	458	A–C	A-1	
$NdFe_{10}Mo_2$	232*	−95*	−67*	57*	147	A–C	A-1	Low $H_A(T)$
$NdFe_{10}Mo_2N$	1175	25	−632	690	501	A–C	A-1	
$NdFe_9Mo_3$	⋯	⋯	⋯	⋯	130	A–C	⋯	Low $H_A(T)$
$NdFe_9Mo_3N$	948	83	−699	521	402	A–C	A-1	

constant K_1 is positive above and below T_s due to high uniaxial Fe anisotropy in spite of the negative contributions from A_{20} and A_{40}. So, the SRT in $NdFe_{11}Mo$ differs from the continuous SRT in $NdFe_{10}Mo_2$,[2] which occurs due to a competition of the Fe and Nd contributions to K_1. The calculated curves of $H_A(T)$ as well as the experimental $H_A(T)$ for $NdFe_{11}Mo$ using the fitted crystal and exchange field parameters are shown in Fig. 2. The calculated $H_A(T)$ increases considerably at low temperatures due to contributions of the fourth and sixth CEF terms as calculated for $NdFe_{10}Mo_2$.[2] The relative error ϵ of the linear theory is not large for all temperatures and has a small value (<0.03) within the temperature region where H_A was measured. The reason for the small values of $H_A(T)$ measured above T_s is the small values of the sum $K_1+2K_2+3K_3$ within 150–400 K.

By fitting the experimental data as obtained for $NdFe_{11}MoN$ a set of crystal field parameters $T_{ex}=1140$, $A_{20}=51$ K, $A_{40}=-611$ K, $A_{60}=710$ K was calculated. The experimental values of $H_A(T)$ were used for the fits using a least-squares procedure. All CEF and exchange field parameters after nitrogenation changed drastically compared with $NdFe_{11}Mo$. The main differences with the set for $NdFe_{11}Mo$ are as follows: (1) T_{ex} increased, leading to an increase of T_C; (2) A_{20} is positive. The type of SRT, FOMP, and T_s also changed.

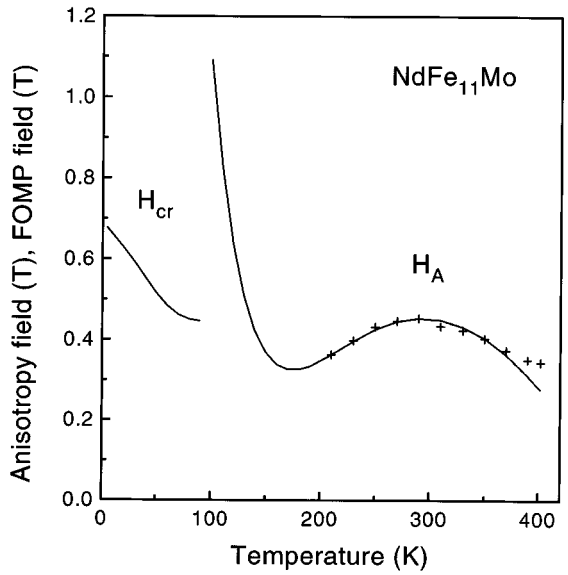

FIG. 2. Temperature dependence of the FOMP field and the anisotropy field for $NdFe_{11}Mo$. The solid line represents the calculated values, the crosses (+) the experimental values.

The calculated cone angle $\theta_c(T)$ in $NdFe_{11}MoN$ increases continuously with decreasing temperature and the SRT predicted at $T_s=458$ K is of second order. The calculated value of $\theta_c(4.2\text{ K})$ is 55°. The present set of the Nd^{3+} crystal field parameters leads to the prediction of a type-1 FOMP in axial fields at low temperatures. The calculated FOMP field increased by approximately a factor of 10 in comparison with $NdFe_{11}Mo$ (Fig. 3).

With the fitted crystal field parameters the anisotropy constant K_2 is positive at high temperatures and negative at low temperatures and K_3 is positive over the whole temperature range for $NdFe_{11}MoN$ due to a considerable value $\theta_6<0$. The Fe sublattice and the CEF parameters A_{20}, A_{60} give a positive contribution to $K_1(T)$. But the first anisotropy constant K_1 changes its sign from positive to negative at T_s due to negative contributions of A_{40}. At low temperatures, when the contribution from A_{60} will be leading, $K_1(T)$ changes the sign to positive again. So, the SRT easy axis–easy cone in $NdFe_{11}MoN$ differs from the SRT in $NdFe_{11}Mo$, which should occur at $K_1(T)>0$. The calculated curves of $H_A(T)$ as well as the experimental $H_A(T)$ for $NdFe_{11}MoN$ using the fitted crystal and exchange field parameters are shown in Fig. 3. The relative error ϵ (4) of the linear theory is small for all temperatures.

C. $NdFe_{10}Mo_2N$ and $NdFe_{10}Mo_2$

Fitting the experimental data of $H_A(T)$ for $NdFe_{10}Mo_2$ a set of rare-earth ion parameters are deduced in Ref. 4: $A_{20}=-95$ K, $A_{40}=-67$ K, $A_{60}=57$ K. The equation $K_1(T_s)=0$, the exchange-field parameter $T_{ex}=232$ K, and the experimental values of $H_A(T)$ for the fitting procedure were used. The calculated cone angle θ_c in $NdFe_{10}Mo_2$ changes continuously with decreasing temperature and the SRT observed at $T_s=147$ K is of second order. The first anisotropy constant K_1 is positive above $T_s=147$ K and changes the sign at T_s with decreasing temperature due to negative contributions of A_{20} and A_{40}. So, the SRT in $NdFe_{10}Mo_2$ occurs due to a competition of the Fe and Nd contributions to K_1.

Fitting the experimental data of $H_A(T)$ for $NdFe_{10}Mo_2N$ a set of Nd^{3+}-ion parameters are calculated: $T_{ex}=1175$ K, $A_{20}=25$ K, $A_{40}=-632$ K, $A_{60}=690$ K. The equation $K_1(T_s)=0$ and the experimental values of $H_A(T)$ were used

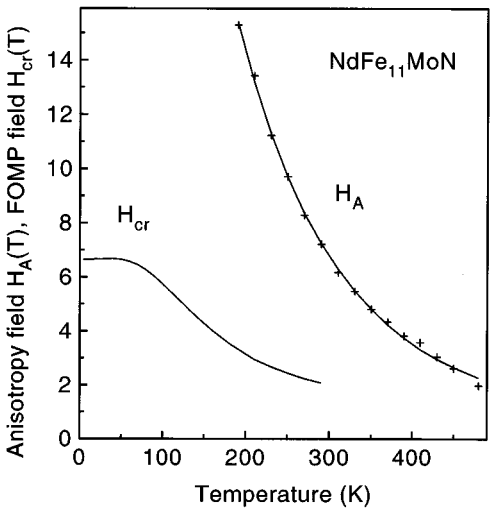

FIG. 3. Temperature dependence of the FOMP field and the anisotropy field for $NdFe_{11}MoN$. The solid line represents the calculated values, the crosses (+) the experimental values.

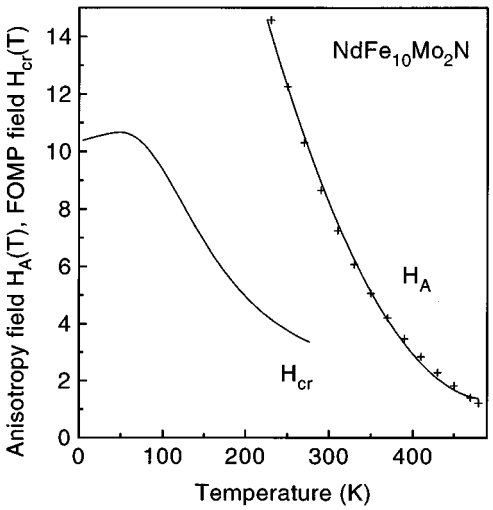

FIG. 4. Temperature dependence of the FOMP field and the anisotropy field for $NdFe_{10}Mo_2N$. The solid line represents the calculated values, the crosses (+) the experimental values.

for the fitting procedure. The calculated cone angle θ_c in $NdFe_{10}Mo_2N$ changes continuously with decreasing temperature and the SRT predicted at $T_s=501$ K is of second order. In comparison with $NdFe_{10}Mo_2$, T_{ex} increased and A_{20} has changed to a positive value. The parameters $|A_{40}|$, $|A_{60}|$ increased without changing the signs. The crystal field parameters calculated within this work are shown in Table I.

The first anisotropy constant K_1 is positive above $T_s=501$ K and changes the sign at T_s with decreasing temperature due to negative contributions of A_{40}. The contribution from A_{60} will be leading at low temperatures and $K_1(T)$ changes its sign at 174 K to positive again. This change does not lead to a SRT and $\theta(T)$ remains continuous. The SRT in $NdFe_{10}Mo_2N$ occurs due to a competition of the Nd contributions to K_1 from different CEF terms. The calculated $H_A(T)$ and $H_{cr}(T)$ as well as the experimental $H_A(T)$ for $NdFe_{10}Mo_2N$ are shown in Fig. 4. The relative error of the linear theory $\epsilon(T)$ is negligible over the whole temperature range.

D. $NdFe_9Mo_3N$ and $NdFe_9Mo_3$

The temperature dependence of H_A was not detectable for $NdFe_9Mo_3$ (Ref. 4) by the SPD technique. The reason for this is, probably, a very low or planar anisotropy within a wide temperature area. A SRT at $T_s=130$ K was detected by ac susceptibility measurements[4] in this compound. A set of crystal field parameters: $T_{ex}=948$ K, $A_{20}=83$ K, $A_{40}=-699$ K, $A_{60}=521$ K (Table I) were obtained by applying Eqs. (2)–(5) on the experimental data[4] for $NdFe_9Mo_3N$. A type-1 FOMP in an axial magnetic field is predicted with these parameters at low temperatures.

The CEF parameters A_{20}, A_{60} give positive contributions and A_{40} gives a negative contribution to K_1. The first anisotropy constant K_1 changes its sign from positive to negative at $T_s=402$ K due to negative contributions of A_{40}. At low temperatures, when the contribution from A_{60} will be leading, $K_1(T)$ changes its sign to positive again. The anisotropy constant K_3 is positive over the whole temperature range. The calculated anisotropy constant K_2 is positive at high temperatures and negative (due to a negative contribution of A_{60}) at low temperatures. The calculated $H_A(T)$ and $H_{cr}(T)$ as well as the experimental $H_A(T)$ for $NdFe_9Mo_3N$ are shown in Fig. 5. $H_A(T)$ has a considerable high value at low temperatures. The $\epsilon(T)$ is negligible for $NdFe_9Mo_3N$ over the whole temperature range.

The temperature dependencies of the anisotropy fields in $NdFe_{12-x}Mo_xN$ ($x=1,2,3$) are the same (after scaling to T_C). The values of H_A are high due to positive contributions of all CEF parameters A_{no} to $H_A(T)$. Based on present calculations, the easy axis–easy cone SRT calculated in $NdFe_{12-x}Mo_xN$ occurs due to $K_1(T)=0$ at T_s above room temperature. A_{40} is the leading parameter in determining the SRT near the transition temperatures T_s. A SRT occurs due

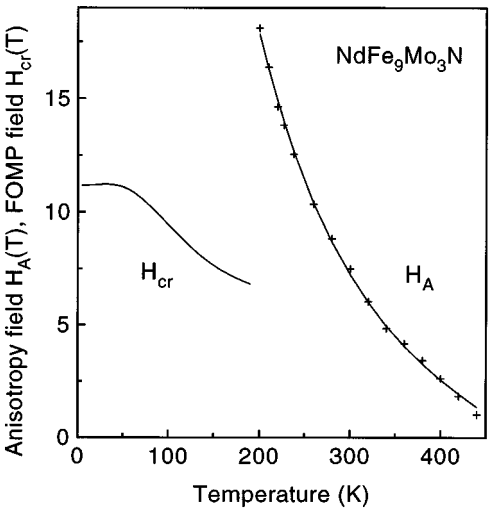

FIG. 5. Temperature dependence of the FOMP field and the anisotropy field for $NdFe_9Mo_3N$. The solid line represents the calculated values, the crosses (+) the experimental values.

to a negative contribution of A_{40} to $K_1(T)$. The calculated parameters A_{20} are positive and the Nd–Fe intersublattice exchange coupling (T_{ex}) increases for the $NdFe_{12-x}Mo_xN$ series compared with $NdFe_{12-x}Mo_x$. Not only the Fe–Fe exchange coupling[8,10] but also the Nd–Fe coupling (T_{ex}) increases because of the nitrogenation. The possible reason for this is an increase of the Fe-sublattice magnetization. The last conclusion contradicts the supposition of Ref. 14 that Nd–Fe interaction decreases by nitrogenation.

In order to estimate the influence of nitrogen on the CEF parameters we use the superposition model[20] and bonding-charge model.[11] Within these models the concentration dependence of A_{20} can be written as follows:

$$A_{20}(y)=A_{20}(0)+y\Delta A_{20},$$
$$\Delta A_{20}=b_2(R)=-e^2\frac{Q}{R^3}\langle r^2\rangle_{\mathrm{Nd}}, \tag{8}$$

where y is the number of nitrogen atoms per formula unit in $NdFe_{12-x}Mo_xN_y$, $R=c/2$ is the distance between Nd and N ions, Q is the effective charge located at the N ion lattice site in units of electron charge.

Using the fitted CEF parameters shown in Table I and $y=1.3$ for $x=1$ and $y=0.9$ for $x=2$,[4] one can find that $\Delta A_{20}=168$ K for $NdFe_{11}MoN$ and $\Delta A_{20}=133$ K for $NdFe_{10}Mo_2N$. These ΔA_{20} values are less than the calculated ones for $NdFe_{11}TiN$ (Ref. 11) and $SmFe_{11}TiN$ compounds. A positive shift of $A_{20}(y)$ means that within the point charge model Q will be negative. We calculate $Q=-4.5\times10^{-2}$ for $x=1$ and $Q=-3.7\times10^{-2}$ for $x=2$, which agrees with the bonding-charge model picture. One can calculate using the bonding-charge model that the expected N-ion charges are $Q=-0.26$ ($x=1$, $c/2=2.40$ Å) and $Q=-0.23$ ($x=2$, $c/2=2.45$ Å) with the model parameters given in Ref. 11. This big difference arises due to strong screening from the $5s$ and $5p$ electron shells of Nd ions in these intermetallics. Using $Q<0$ leads to the prediction $\Delta A_{40}>0$ and $\Delta A_{60}>0$ within the point charge model. But the ΔA_{40} signs are in contradiction to our previous analysis, where $\Delta A_{40}<0$ was calculated for $NdFe_{12-x}Mo_xN$ (Table I). The point charge model cannot explain even the signs of the shifts ΔA_{no}.

The contribution of Nd–Fe exchange coupling to the Curie temperature can be estimated within the two-sublattice molecular field theory as follows:

$$T_C=\frac{1}{2}\left[T_{\mathrm{Fe}}+(T_{\mathrm{Fe}}^2+4T_{\mathrm{NdFe}}^2)^{1/2}\right],$$
$$T_{\mathrm{NdFe}}=\frac{1}{3}\,|g_J-1|\left(\frac{J(J+1)(S^*+1)}{(12-x)S^*}\right)^{1/2}T_{\mathrm{ex}}, \tag{9}$$

where T_{Fe} is the Curie temperature of the isostructural Y compounds, S^* is an effective Fe-ion spin, which can be calculated from the Fe magnetization $M_{\mathrm{Fe}}(4.2\ \mathrm{K})=2N_{\mathrm{Fe}}\mu_{\mathrm{B}}S^*$ [$N_{\mathrm{Fe}}=(12-x)$ per f.u.].

The calculated T_{NdFe} by Eq. (9) increases whereas T_{Fe} decreases with increasing x. $M_{\mathrm{Fe}}(x)$ also decreases. This means a general increase of the relative role of the Nd sublattice in $NdFe_{12-x}Mo_xN$ series with increasing x and this result agrees with Ref. 14.

V. SUMMARY

The easy axis–easy cone spin–reorientation transitions in $NdFe_{11}Mo$ and $NdFe_{10}Mo_2$ detected at $T_s=168$ and 147 K in Ref. 4 are due to our fitted CEF and exchange field parameters of first ($x=1$) and second order ($x=2$), respectively. The angle between $\mathbf{M}_s$ and the c axis increases continuously with decreasing temperature below T_s for $x=2$ and exhibits a jump for $x=1$. A type-2 FOMP at low temperatures is predicted for $NdFe_{11}Mo$ applying a magnetic field perpendicular to the alignment direction. High anisotropy fields are calculated for $NdFe_{11}Mo$ at low temperatures. The SRT and FOMP in $NdFe_{11}Mo$ and $NdFe_{10}Mo_2$ are a consequence of the dominant contributions of the high order CEF terms to the rare-earth anisotropy.

For all $NdFe_{12-x}Mo_xN$ intermetallics a SRT easy axis–easy cone of second order is calculated below the Curie temperatures. A type-1 FOMP at low temperatures is predicted for $NdFe_{12-x}Mo_xN$ ($x=1,2,3$) when a magnetic field is applied parallel to the c axis. These SRTs and FOMPs are determined by the fourth- and sixth-order CEF terms. The point charge model cannot predict the change of A_{no}. The change of the CEF due to nitrogenation can be described within the crystal-field-superposition model.

The calculated curves of $H_A(T)$ for $NdFe_{12-x}Mo_xN$ ($x=1,2,3$) are in good agreement with the experimental curves over a wide temperature range. The temperature dependence of the FOMP critical fields $H_{\mathrm{cr}}(T)$ are calculated for $NdFe_{12-x}Mo_xN$ ($x=1,2,3$).

ACKNOWLEDGMENTS

This work was supported by the ''Fond zur Förderung der Wissenschaftlichen Forschung von Österreich'' under Grant Nos. S5604, S5605. K.Yu.G. thanks the ''Fond zur Förderung der Wissenschaftlichen Forschung'' of Austria for financial support by Lise-Meitner Stipendium under Project No. M00175-PHY.

[1] K. Yu. Guslienko, X. C. Kou, E. H. C. P. Sinnecker, and R. Grössinger (unpublished).
[2] K. Yu. Guslienko, X. C. Kou, and R. Grössinger, J. Magn. Magn. Mater. **150**, 383 (1995).
[3] H. Sun, Y. Morii, H. Fujii, M. Akayama, and S. Funahashi, Phys. Rev. B **48**, 13333 (1993).
[4] E. H. C. P. Sinnecker, X. C. Kou, and R. Grössinger, IEEE Trans. Magn. (in press).
[5] M. Anagnostou, C. Christides, M. Pissas, and D. Niarchos, J. Appl. Phys. **70**, 6012 (1991).
[6] Y. Z. Wang, B. P. Hu, X. L. Rao, G. C. Liu, L. Yin, W. Y. Lai, W. Gong, and G. C. Hadjipanayis, J. Appl. Phys. **73**, 6251 (1993).
[7] Z. X. Tang, W. Singleton, and G. C. Hadjipanayis, J. Appl. Phys. **73**, 6254 (1993).
[8] H. Sun, M. Akayama, K. Tatami, and H. Fujii, Physica B **83**, 33 (1993).
[9] H. Sun, M. Akayama, and H. Fujii, Phys. Status Solidi A **140**, K107 (1993).
[10] Y. Z. Wang, B. P. Hu, L. Song, K. Y. Wang, and G. C. Liu, J. Phys.: Condens. Matter **6**, 7085 (1994).
[11] Y. Z. Wang, L. Song, K. Y. Wang, G. C. Liu, and W. Y. Lai, J. Magn. Magn. Mater. **140–144**, 1019 (1995).
[12] H. S. Li and J. M. Cadogan, J. Magn. Magn. Mater. **109**, L153 (1992).
[13] R. Skomski, M. D. Kuz'min, and J. M. D. Coey, J. Appl. Phys. **73**, 6234 (1993).

[14] J. Yang, S. Dong, W. Mao, P. Xuan, Y. Yang, and S. Ge, J. Appl. Phys. **78**, 1140 (1995).
[15] R. Lorenz, J. Hafner, S. S. Jaswal, and D. J. Sellmyer, Phys. Rev. Lett. **74**, 3688 (1995).
[16] Y. Z. Wang, B. P. Hu, X. L. Rao, G. C. Liu, L. Song, L. Lin, and W. Y. Lai, J. Appl. Phys. **75**, 6226 (1994).
[17] M. D. Kuz'min, and J. M. D. Coey, Phys. Rev. B **50**, 12533 (1994).
[18] G. Asti and F. Bolzoni, J. Magn. Magn. Mater. **20**, 29 (1980).
[19] D. J. Newman and B. Ng, Rep. Prog. Phys. **52**, 699 (1989).
[20] B. P. Hu, H. S. Li, and J. M. D. Coey, J. Appl. Phys. **67**, 4838 (1990).
[21] G. Asti and S. Rinaldi, J. Appl. Phys. **45**, 3600 (1974).
[22] C. V. Thang, P. Thuy, N. M. Hong, T. D. Hien, N. S. Almodova, and R. Grossinger, J. Magn. Magn. Mater. **140–144**, 1017 (1995).